Journal of Cell Science 113, 1589-1600 (2000)
Printed in Great Britain © The Company of Biologists Limited 2000
JCS0942

Glycocalyx modulation is a physiological means of regulating cell adhesion

Siham Sabri, Mireille Soler, Colette Foa, Anne Pierres, Anne-Marie Benoliel and Pierre Bongrand*

Laboratoire d'Immunologie, INSERM U 387, Hôpital de Sainte-Marguerite, BP 29, 13274 Marseille Cedex 09, France
*Author for correspondence (e-mail: bongrand@marseille.inserm.fr)

Accepted 17 February; published on WWW 6 April 2000

SUMMARY

Here we present experimental evidence that phagocytic cells use modulation of specific components of their glycocalyx to regulate their binding capacity.

Particles coated with antibodies specific for the CD32 medium affinity IgG receptor were driven along human monocytic THP-1 cells (expressing CD32) in a flow chamber operated at low shear rate. Surprisingly, only minimal adhesion was observed. However, when cells were activated by exposure to fibronectin-coated surfaces and/or soluble gamma interferon, adhesion efficiency was dramatically increased, whereas the apparent glycocalyx thickness displayed 20% decrease, and the surface density of CD43/leukosialin carbohydrate epitopes displayed 30-40% decrease on activated cells.

The existence of a causal link between adhesion increase and glycocalyx alteration was strongly supported by the finding that (i) both phenomena displayed similar kinetics, (ii) an inverse relationship between THP-1 cell binding capacity and glycocalyx density was demonstrated at the individual cell level, and (iii) adhesion enhancement could not be ascribed to an increased binding site density or improved functional capacity of activated cells.

Additional experiments revealed that cell-to-particle adhesion resulted in delayed (i.e. more than a few minutes) egress of CD43/leukosialin from contact areas. Since the time scale of particle attachment was less than a second, surface mobility should not affect the potential of CD43 to impair the initial step of adhesion.

Finally, studies performed with fluorescent lectins suggested that THP-1 cell activation and increased adhesive potential were related to a decrease of O-glysosylation rather than N-glycosylation of surface glycoproteins.

Key words: Glycocalyx, Cell coat, Flow chamber, Anti-adhesion, THP-1 cell, Activation, CD32, CD43

INTRODUCTION

Cell function requires a tight control of adhesive interactions. Thus, rapid transition between nonadherent and adherent states is of key importance to leucocyte behaviour (Springer, 1990a).

Numerous mechanisms are used by living cells to regulate adhesion (Pierres et al., 1998a), including modulation of surface receptor density (Bevilacqua and Nelson, 1993), affinity (Loftus and Liddington, 1997) or kinetic parameters (Cai and Wright, 1995) and alteration of the mobility (Stewart et al., 1998; Yauch et al., 1997) or topographical distribution of these receptors on cell membranes (Yap et al., 1997).

While all these mechanisms are well suited to regulate the activity of a precise receptor species, many experimental results support the hypothesis (Rutishauser et al., 1988) that cells may control their overall adhesive capacity by modulating the density of the potentially repulsive peripheral structure denominated as the glycocalyx (Bennett, 1963), cell coat (Leblond and Bennett, 1974) or pericellular matrix (Lee et al., 1993). A prominent example is the large (i.e. 45 nm long) molecule called CD43 or leukosialin that is found on most leucocytes (Remold O'Donnell et al., 1984; Cyster et al., 1991). Leukosialin is thought to be a fairly rigid and extended molecule, due to the high density of O-linked sugars (Cyster et al., 1991; Jentoft, 1990). This is thought to contribute a significant part of the leucocyte glycocalyx due to both its size and abundance (Brown et al., 1981; Ostberg et al., 1998). Indeed, it might cover as much as 10% of the cell area (Brown et al., 1981). Ardman et al. (1992) reported decreased adhesiveness in transfected HeLa cells overexpressing CD43. Conversely, cells with defective expression of CD43 exhibited increased adhesiveness (Manjunath et al., 1995; Stockton et al., 1998). Finally, when leucocytes were subjected to physiological stimuli such as chemotactic peptides, chemokines or cytokines, they displayed both alteration of CD43 expression and increased adhesiveness (Rieu et al., 1992).

However, some points must be clarified to demonstrate that the modulation of glycocalyx elements, and particularly CD43, is a physiological means of regulating cell adhesion. First, the experimental demonstration that cell adhesiveness was increased following removal of membrane components often involved fairly drastic and unphysiological procedures such as gene manipulation (Ardman et al., 1992; Manjunath et al., 1995; Stockton et al., 1998), metabolic inhibitors (Patel et al., 1995) or enzymatic treatment (Sabri et al., 1995). Second, since leucocytes may express more than 60 species of adhesion receptors (Barclay, 1998), it is often difficult to rule out the possibility that CD43 might influence cell adhesion through negative regulation of some unidentified receptor. Indeed,

CD43 is endowed with signaling potential (Silverman et al., 1989). Third, it was recently demonstrated with fluorescence (Soler et al., 1997; Sperling et al., 1998) or electron (Soler et al., 1997, 1998) microscopy that CD43 and/or cell surface carbohydrates might exit from cell adhesion areas following contact formation. This phenomenon might minimize the anti-adhesive potential of bulky cell surface molecules.

The aim of the present study was to assess the role of glycocalyx alteration in the increased binding of model particles interacting with well-defined receptors of human phagocytic cells exposed to physiological stimuli. We used the human monocytic line THP-1 (Tsuchiya et al., 1982) as a suitable model of monocyte-macrophage differentiation (Auwerx, 1991; Schwende et al., 1996). Cells were made to bind spheres coated with monoclonal antibodies specific for the CD32 medium affinity IgG receptor. We compared the cellular uptake of soluble antibodies and antibody-coated particles, in order to discriminate between intrinsic and 'perireceptor' parameters. Glycocalyx modulation was achieved by exposing cells to fibronectin, a constituent of extracellular matrices possibly involved in monocyte activation (Lukacs et al., 1995) and interferon gamma, a major activator of mononuclear phagocytes (Adams and Hamilton, 1984). Instead of assaying adhesion under static conditions, i.e. by letting particles fall on adherent monocytes, thus allowing a contact time of several minutes, dynamic particle uptake was studied: we monitored the uptake of slowly moving particles encountering monocytes in a laminar flow chamber operated as very low shear rate. The contact time was thus of order of a second. This allowed us to test the initial step of adhesion without interference with further metabolically-dependent processes that might be affected by cell activation (Pierres et al., 1994; Sabri et al., 1995). Conventional and confocal microscopy were used to study the density and distribution of glycocalyx elements, and particularly CD43, on control and activated cells. Cell activation triggered both a decrease of glycocalyx density and an increase of dynamic binding efficiency. Both events displayed similar kinetics, and they were correlated at the individual cell level. Finally, it was found that CD43 depletion from adhesion areas did not occur during the first minutes following contact formation. It is concluded that glycocalyx modulation is indeed used by living cells to modulate adhesion under physiological condition. Delayed redistribution of potentially repulsive molecules might play a role in later steps of the adhesive process.

MATERIALS AND METHODS

Cells and culture

The human monocytic THP-1 line (Tuschiya et al., 1982) was a kind gift from Dr F. Birg (INSERM U 119, Marseille). Cells actively ingested opsonized erythrocytes and displayed expected antigens (including CD11b, CD18, CD35, CD64) as assayed with flow cytometry (Sabri et al., 1995). Cells were maintained in RPMI 1640 medium (Flow Laboratories, McLean, VA) supplemented with 20 mM HEPES, 20 μM 2-mercaptoethanol, 10% fetal calf serum (Flow), 2 mM L-glutamine, 50 U/ml penicillin and 50 μg/ml streptomycin. Proper differentiation was achieved as previously described (Tsuchiya et al., 1982; Auwerx, 1991) by 18 hours exposure to 10 ng/ml phorbol myristate acetate (Sigma, St Louis, MO). In some cases, recombinant human interferon gamma (Pepro Tech, supplied by TEBU, Houdan, France) was added at a final concentration of 100 U/ml during the last 24 hours preceding adhesion tests. Interferon gamma is essentially identical to 'macrophage activating factor' whose role is to enhance the activity of dormant macrophages and induce a so-called 'primed state' with increased capacity to kill many pathogens (Adams and Hamilton, 1992). In some experiments, cells were incubated for 30 minutes at 37°C in culture medium supplemented with 150 μg/ml O-sialoglycoprotein endopeptidase from *Pasteurella haemolytica* (EC3.4.24.57, supplied by Valbiotech, Paris) to remove O-linked oligosaccharides. They were then washed twice and used immediately for adhesion assay or flow cytometry.

Particles

Particles were tosyl-derivatized spheres of 2.8 μm diameter (Dynabeads M-280, supplied by Dynal France, Compiègne). Fifty microliter aliquots (about 30 million beads) were added to 50 μl of a 200 μg/ml solution of murine IgG1 monoclonal antibodies (anti-CD32, specific for the low affinity FcγRII immunoglobulin receptor, from clone AT10, supplied by Serotec, Besançon, France, or IgG1 isotypic control provided by Immunotech, Marseille). It was important to use an IgG1 since this immunoglobulin class is only weakly bound by the CD64 high affinity FcγRI immunoglobulin receptor. Buffer was 0.05 M borate, pH 9.5. Samples were incubated for 24 hours at 37°C in a rotating agitator, then washed extensively in pH 7.2 phosphate buffer solution before adhesion tests.

Adhesion (static conditions)

Glass sheets (22×11 mm^2) were cut out of coverslips and washed with ethanol, then sterilized. In some cases, they were incubated with PBS containing 10 μg/ml human plasma fibronectin (Sigma) for one hour at room temperature. Fibronectin is known to interact with phagocyte integrin receptors such as $\alpha_4\beta_1$ and $\alpha_5\beta_1$ that are expressed by THP-1 cells (not shown). This interaction was shown to enhance complement-mediated phagocytosis by human monocytes (Wright et al., 1983). This might be a physiological stimulus for blood monocytes, which would appear when fibronectin is uncovered by local alteration of endothelial cells (Lukacs et al., 1995). THP-1 cells (0.5×10^6) were deposited on these sheets and incubated with 10 ng/ml PMA to promote differentiation. They were then washed and 400 μl of particle suspension (0.5×10^6 particles) were deposited in RPMI 1640 medium supplemented with 1g/l BSA (Sigma). Coverslips were incubated for 15 minutes at room temperature and washed with one minute vortexing in 36-mm plastic Petri dishes. Cells were then examined microscopically to determine the number of free and particle-bound cells, and attached particles. Adhesion efficiency was expressed as the percentage of cells binding at least one particle. More than 90% of the glass surface was covered with cells. At least 200 cells were recorded in each determination.

Adhesion (dynamic conditions)

Our procedure was previously described (Pierres et al., 1994; Sabri et al., 1995). Briefly, glass sheets bearing THP-1 monolayers were bound to the bottom of a Plexiglas block (20×12×45 mm^3) bearing a rectangular cavity of 17×6×1 mm^3. Particles were suspended at 2.5×10^6 per ml in RPMI 1640 medium supplemented with 1g/l BSA; they were then driven into the chamber with a 1-ml syringe mounted on an electric syringe holder (Razel Scientific Instruments, suppplied by Bioblock, Illkirch, France). The wall shear rate G was calculated according to the standard formula $G=6Q/h^2w$, where Q is the flow rate (in cm^3/second), and h and w are the chamber height and width, respectively (expressed with the same cm unit). G is thus expressed in $seconds^{-1}$.

The chamber was set on the stage of an inverted microscope (Olympus IM) equipped with a SIT videocamera (Lhesa 4025, Cergy Pontoise France). Observation was performed with a ×100 immersion lens and experiments were recorded with a VHS tape recorder for delayed analysis.

In each experiment, a microscope field was selected and a wall shear rate of 22 seconds^{-1} was maintained for about 10 minutes. All spheres entering the microscope field in contact with the cell monolayer (as evidenced by irregular motion and low velocity) were monitored and the fraction of particles exhibiting a detectable arrest (i.e. more than about 1 second) was determined during their passage through the microscope field (about 86 μm width). Essentially all detected arrests lasted more than 1 minute, and most of them lasted throughout the entire observation period.

Flow cytometry

Immunolabeling was performed by incubating aliquots of 10^6 cells for 30 minutes at 4°C with 10 μg/ml FITC-labeled monoclonal antibodies (anti-CD32, clone AT10, provided by Serotec, or control IgG1, provided by Coulter) in RPMI supplemented with 1g/l BSA. They were then washed three times and fixed with 1% paraformaldehyde before being assayed with a flow cytometer (Epics Profile, Coulter Corp., Hialeah, FLA). Absolute calibration was performed as previously described (Pierres et al., 1994). Briefly, calibrated fluorescent beads (Flow Cytometry Research Corp., Research Triangle Park, North Carolina) were assayed together with labeled cells using flow cytometry. Fluorescent antibodies were then calibrated by studying with a confocal laser scanning microscope (CLSM, Leica, Heidelberg, Germany) a solution of these antibodies deposited as a layer of 10 μm thickness between a glass slide and a coverslip. Beads were also studied and quantitative image processing was used to determine the absolute number of fluorescent antibody molecules yielding the same fluorescence as a calibration bead.

Glycosylation studies were performed by labeling cells with fluorescent lectins (EY Laboratories Inc. (San Mateo, California, USA, supplied by Coger, France). Concanavalin A (from *Canavalia ensiformis*) is known to bind α-D-mannose, α-D-glucose and some branched mannose groups. *Lens culinaris* agglutinin mainly binds α-mannose. Peanut agglutinin (from *Arachis hypogeae*) was used to label terminal β galactose groups. Finally, *Sambucus nigra* agglutinin is specific for α2,6 linked sialyl groups. All lectins were used at 100 μg/ml.

Fluorescent labeling for microscopic studies

Indirect labeling was performed as follows: cells were first incubated for 30 minutes at 4°C with IgG1 monoclonal antibodies. Clone DFT1 (supplied by Immunotech, Marseille, France) was used at 20 μg/ml. This antibody recognized a sialylated epitope of CD43/leukosialin. L10 (a kind gift from Dr Remold O'Donnell recognizing a sialyl-independent epitope of CD43; Remold O'Donnell et al., 1984; Remold O'Donnell and Rosen, 1990) was used at 10 μg/ml. Anti-CD18 clone 7E4 (Immunotech, Marseille) was used at 10 μg/ml. Cells were then washed in PBS supplemented with 1% bovine albumin and incubated for 30 minutes at 4°C with 5 μg/ml biotinylated goat anti-mouse immunoglobulin $(Fab')_2$. They were washed and incubated another 30 minute period at 4°C with 5 μg/ml fluoresceinated streptavidin (Immunotech). Finally, they were washed and stored in washing buffer supplemented with 2% paraformaldehyde.

Absolute calibration and kinetic studies were performed by labeling cells with 20 μg/ml fluorescein-conjugated DFT1 monoclonal antibodies supplied by Sigma.

When cells were labeled after exposure to anti-CD32-coated spheres in the flow chamber, samples were first incubated for 30 mn at 4°C with 10 μg/ml goat anti-mouse immunoglobulin $(Fab')_2$ (Immunotech) to block putative epitopes expressed by anti-CD32 antibodies coupled to the spheres.

Fluorescence microscopy

The fluorescence of adherent cells was quantified as previously described (André et al., 1990). Briefly, cells were examined with an Olympus IMT2 microscope bearing a SIT videocamera (Lhesa 4036, Cergy Pontoise, France). The video output was processed with a PCVision+ digitizer (Imaging Technology, supplied by Imasys, Suresnes, France) mounted on a desk computer, yielding 512×512 pixel images with 256 grey levels. Images were analyzed with a software written in the laboratory. This allowed determination of individual cell contours with a standard boundary-follow algorithm and calculation of total fluorescence intensity with automatic background subtraction. The linearity of fluorescence determinations was checked as previously described (André et al., 1990).

Confocal microscopy

A chamber of about 30 μm thickness was constructed by depositing two parallel strips of aluminium foil on a glass coverslip (22×22 mm^2) bearing adherent THP-1 cells, then glueing another coverslip. The chamber was deposited on the stage of a confocal microscope (CLSM, Leica, Heidelberg) using a ×40 dry objective (P1 Fluotar, 0.70 NA). A suspension of anti-CD32-derivatized spheres was injected. A field was selected and images were recorded every minute for about twenty minutes. The weak fluorescence of spheres allowed clear identification of cells on which spheres fell during the experiment. The isotropy of fluorescence distribution was quantified as previously described (Soler et al., 1997) by dividing the images of individual cells into 6 sectors of angle $\pi/3$ starting from the centroid of the fluorescence distribution and calculating the mean fluorescence of these sectors.

Scanning electron microscopy

Cells were made to bind particles in the flow chamber. Coverslips were then removed and samples were fixed with 2.5% glutaraldehyde in 0.1 M cacodylate buffer (pH 7.4) and postfixed with an aqueous solution of 1% OsO_4. They were then dehydrated with graded ethanol solutions and dried in a Balzer critical point CO_2 apparatus. The samples were placed in a JFC-1100 (Jeol, Japan) sputter coater for coating with gold-palladium. Observation was performed in a Jeol JEM 35CF scanning electron microscope operated at 25 kV.

Transmission electron microscopy

Glycocalyx labeling was obtained with electron-dense cationic dyes (Martinez-Pàlomo, 1970). We used a modification of the lanthanum technique (Revel and Karnovsky, 1967) following Wagner and Chen (1990) who replaced lanthanum with terbium, another lanthanide element yielding improved constrast with conventional electron microscopy. Cells were fixed one hour at room temperature in cacodylate buffer (0.05 M) pH 7.4 containing 2.5% glutaraldehyde (Polysciences, Warrington, PA) and 0.34 M terbium chloride (Wagner and Chen, 1990). Cells were then rinsed three times for 20 minutes each in the same buffer under rotative agitation. They were then incubated for one hour at room temperature in 1% OsO_4 in cacodylate buffer. After rapid dehydration in a graded series of alcohols, cells were embedded in Araldite resin (Polysciences). Sections were cut on a diamond knife and observed without any counterstaining with a 400C Jeol transmission electron microscope.

Analysis of electron microscopic images

Our methodology was previously described (Foa et al., 1994, 1996). Twenty thousandfold enlarged images were digitized with a scanner operated at 400 dpi resolution with 8-bit accuracy (Scanman, Logitech SA, Morges, Switzerland). Pixel size was thus about 3.2 nm. Cell contours were divided in segments of about 800 nm length. Terbium-stained areas were manually delimited, and the local glycocalyx thickness was determined for each pixel with a specific software developed in the laboratory. An average thickness was calculated for each contour segment, and more than 50 segments were averaged to obtain the mean glycocalyx thickness for each studied experimental condition.

Statistical tests

Essentially two procedures were used to estimate the significance of experimental data.

Experiments yielding a quantitative parameter (e.g. mean fluorescence) were repeated several times, and measured values were used for determination of mean and standard error of the mean with conventional formulae. Comparisons were performed with Student's *t*-test, assuming normal distribution.

When a given experiment yielded a frequency (e.g. fraction of monitored particles that were bound in the flow chamber), it was found more rigorous to weight experiments according to the number of counted events: the standard error was calculated as by Snedecor and Cochran (1980):

$$SE = [p(1-p)/n]^{1/2},$$

where n is the number of counted particles and p is the proportion of binding events.

Further, the significance of difference between two frequencies p_1 and p_2 was calculated by assuming a normal distribution for the quantity:

$$z = (p_1 - p_2)/[p(1-p)(1/n_1 + 1/n_2)]^{1/2},$$

where p is the weighted mean, i.e.

$$(p_1 n_1 + p_2 n_2)/(n_1 + n_2).$$

The standard error for the ratio between two frequencies a and b with standard errors α and β (Fig. 5) was then calculated as:

$$(a/b)\,[(\alpha/a)^2 + (\beta/b)^2]^{1/2}$$

(Rosengard, 1972).

RESULTS

CD32 epitopes expressed by THP-1 cells are accessible to particle-bound antibodies under static, not under dynamic conditions

First, anti-CD32 coated spheres were sedimented on glass-adherent THP-1 cells. When unattached spheres were eliminated by prolonged vortexing, about 50% of THP-1 cells bound at least one particle, and this interaction was specific since it was decreased tenfold when anti-CD32 antibodies were replaced with mouse immunoglobulins of similar isotype (Table 1, first row). However, when spheres were driven along THP-1 cells under low hydrodynamic flow, only minimal adhesion occurred, and no signficant difference was found between spheres coated with anti-CD32 antibodies or isotypic controls (Table 1).

The dynamic uptake of anti-CD32-coated spheres is dramatically enhanced when THP-1 cells are cultured on fibronectin-coated surfaces and stimulated with IFN-γ

It was asked whether dynamic adhesion might be increased by proper cell stimulation. Thus, THP-1 cells were cultured on fibronectin-coated surfaces instead of untreated glass, and/or they were stimulated with IFN-γ before adhesion assay. Results of three series of experiments are summarized in Table 1: under static conditions, all THP-1 cells readily bound anti-CD32-coated beads, not IgG1-treated controls. However, dynamic adhesion was markedly dependent on culture conditions. Indeed, when cells were plated on fibronectin instead of bare glass, or when they were stimulated with IFN-γ, adhesion efficiency exhibited about fourfold increase, and this enhancement was specific since the uptake of control spheres was not altered. Also, when fibronectin and IFN-γ were combined, the uptake of anti-CD32-coated beads displayed fivefold increase. Therefore, further experiments were done with IFN-γ-stimulated cells deposited on fibronectin-coated surfaces (these are referred to as 'stimulated'), as compared to control cells deposited on bare glass.

Table 1. Influence of THP-1 cell treatment on adhesion efficiency under static and dynamic conditions

		% Binding cells			
		Static conditions		Dynamic conditions	
Surface	Stimulation	IgG1	Anti-CD32	IgG1	Anti-CD32
Bare glass	None	5.5±1.5	47±6.5	4.0±1.5	7±2.5
Fibronectin	None	6.6±2	43±5	4.5±2	27±7.5
Bare glass	IFN-γ	4.5±1.5	41±8.5	4.6±2.5	29±8.5
Fibronectin	IFN-γ	6.5±14	45.5±5.5	5±2.5	37±10

Monocytic THP1-cells were cultured on bare or fibronectin-coated glass surfaces with or without IFN-γ. They were then exposed to IgG1- or anti-CD32-coated spheres under static or dynamic conditions and examined microscopically for determination of the percent of cells binding to at least one particle. Each result is a mean of 3 separate results ± s.e.m.

However, it was difficult to compare the absolute values of binding frequencies obtained under static and dynamic conditions since the mean number of particles encountered per cell was quite different under both contitions. It was thus felt useful to achieve a more quantitative determination of binding efficiency. Videotapes recorded during flow experiments were replayed in order to monitor *all* spheres and calculate the fraction of these particles that were bound during their passage. As shown in Fig. 1, the influence of cell culture conditions on dynamic adhesion was confirmed since optimal stimulation resulted in tenfold increase of uptake efficiency, as compared to controls.

Dynamic sphere uptake by stimulated THP-1 cell monolayers is a consequence of bona fide adhesive events

It was previously reported that particle uptake by THP-1 cell monolayers might be due to artefactual trapping in regions of low shear appearing as holes between adjacent cells. As shown in Fig. 2, this possibility was ruled out by scanning electron microscopy.

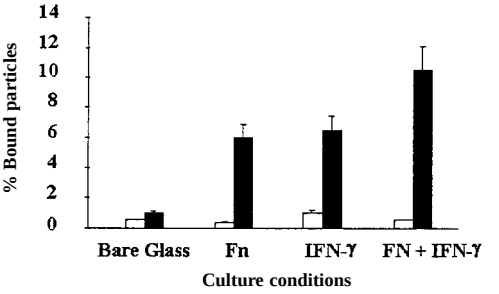

Fig. 1. Influence of THP-1 cell culture conditions on dynamic uptake of antibody-coated beads. Monocytic THP-1 cells were cultured on bare or fibronectin-coated glass, with or without interferon-γ, then exposed to a laminar shear flow in presence of control (white areas) or anti-CD32-coated (black areas) spheres. Individual spheres flowing in contact with THP-1 cells were monitored for detection of binding events. The fraction of flowing spheres exhibiting at least one binding event during their passage was calculated on a population of at least 200 particles, and mean values obtained in five independent experiments are shown. Vertical bar length = s.e.m.

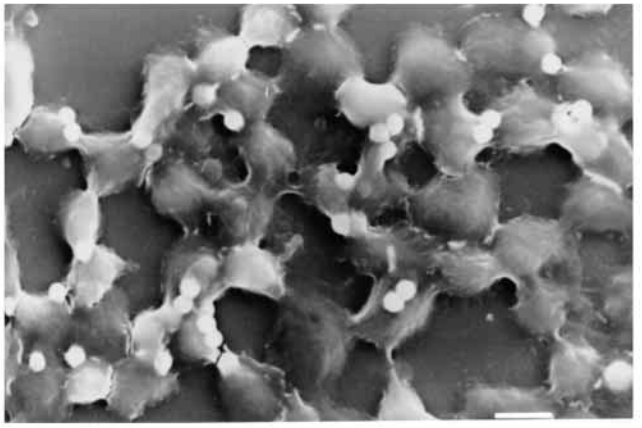

Fig. 2. Cell-particle interaction in the flow chamber. Stimulated THP-1 cells were exposed to moving anti-CD32 coated beads in the flow chamber. They were then fixed and processed for scanning electron microsopy: retained particles where actually deposited on the cell body, suggesting that particle uptake was due to actual adhesion rather than kinetic trapping in regions of lower shear rate. Bar, 10 μm.

The stimulation of dynamic adhesion is not due to a change of CD32 antigen expression on THP-1 cells

A simple explanation of our findings would be that fibronectin or IFN-γ increased the density of CD32 epitopes expressed on THP-1 cells. In order to test this possibility, CD32 expression was assayed with flow cytometry with the same monoclonal antibody as was used for adhesion tests. As shown in Table 2, epitope density was similar on stimulated and control cells.

Further, since adherent mononuclear phagocytes have a well-known capacity to selectively concentrate some receptor subpopulations on their adherent surface (Rabinovitch et al., 1975; Michl et al., 1983), it was important to compare the density of CD32 epitopes on the upper side of adherent control and stimulated THP-1 cells. This was achieved with quantitative immunofluorescence microscopy. As shown in Table 3, control and stimulated THP-1 cells displayed similar labeling intensity when they were stained without being detached from their substratum. Also (not shown), average cell surface area was similar with and without fibronectin or interferon-γ treatment.

Finally, as exemplified in Fig. 3, when the topographical distribution of CD32 was studied on control and stimulated THP-1 cells, the label appeared uniformly distributed on the surface of both cell populations.

Table 2. Influence of culture conditions on CD32 expression by THP-1 cells

Surface	Stimulation	Fluorescence intensity		Number of CD32 (sites/cell)
		IgG1	CD32	
Bare glass	None	0.30	8.35	48,000
Fibronectin	None	0.53	7.92	45,500
Bare glass	IFN-γ	0.61	7.18	41,300
Fibronectin	IFN-γ	0.59	7.79	44,800

Monocytic THP-1 cells were cultured on glass or fibronectin-coated surfaces with or without IFN-γ. They were then detached by gentle mechanical agitation and labeled with fluorescent control IgG1 or anti-CD32 IgG1 for flow cytometry. Each experiment was repeated at least 4 times and a representative set of results is shown.

Table 3. Effect of cell treatment on surface expression of CD32 sites

Cell culture	Mean fluorescence intensity	
	IgG1	Anti-CD32
Control	1.44±0.8	23.63±0.67
Fibronectin + IFN-γ	1.76±1.28	23.60±0.45

Monocytic THP-1 cells were cultured on bare glass in normal culture medium (control) or on fibronectin-coated coverslips in IFN-γ-containing medium. They were then washed and labeled for CD32, then studied with quantitative fluorescence microscopy for mean fluorescence determination. At least 150 separate cells were studied under each condition and mean values are shown ± s.e.m.

THP-1 cell stimulation did not result in substantial morphological alteration

Since adhesion efficiency under flow might be influenced by cell morphological features such as length and density of surface protrusions, control and stimulated cells were compared with scanning electron microscopy. As exemplified in Fig. 4, stimulation with fibronectin and interferon did not result in substantial morphological alteration. Also, adherent cells appeared as relatively smooth with limited amount of surface protrusions.

The stimulation-induced increase of CD32 accessibility in stimulated THP-1 cells is tightly correlated to a decrease of CD43/leukosialin glycosylation

Since CD43 was reported to behave as an anti-adhesive molecule (Ardman et al., 1992) and it was found to be altered through proteolysis (Rieu et al., 1992; Remold O'Donnell and Parent, 1994) or dysglycosylation (Soler et al., 1997) upon leucocyte activation, it was tempting to look for a possible correlation between the higher CD32 accessibility of stimulated THP-1 cells and an alteration of CD43 expression.

This was first tested by comparing the CD43 expression on control and stimulated cells with quantitative

Table 4. Effect of THP-1 cell stimulation on the expression of sialyl-dependent and sialyl-independent epitopes of CD43

Surface	Stimulation	Fluorescence	
		Sialyl-dependent epitope (bound molecules per cell)	Sialyl-independent epitope (relative fluorescence)
Glass	-	57,000±2,700	1.15±0.08
Fibronectin	-	34,300±2,000 (P<0.001)	0.85±0.13 (P≈0.05)
Glass	Interferon-γ	43,400±3,900 (P<0.05)	1.24±0.11 (P>0.05)
Fibronectin	Interferon-γ	38,900±4,100 (P<0.001)	1.10±0.08 (P>0.40)

THP-1 cells were cultivated on bare glass or fibronectin with or without addition of interferon-γ in the culture medium. They were then labeled with anti-CD43 antibodies (specific for a sialyl-dependent or a sialyl-independent epitope) and the mean fluorescence of 19 to 50 separated cells were determined. Mean values are shown ± s.e.m. The significances of the effect of culture conditions on antigen expression were calculated with Student's *t*-test and they are shown in brackets.

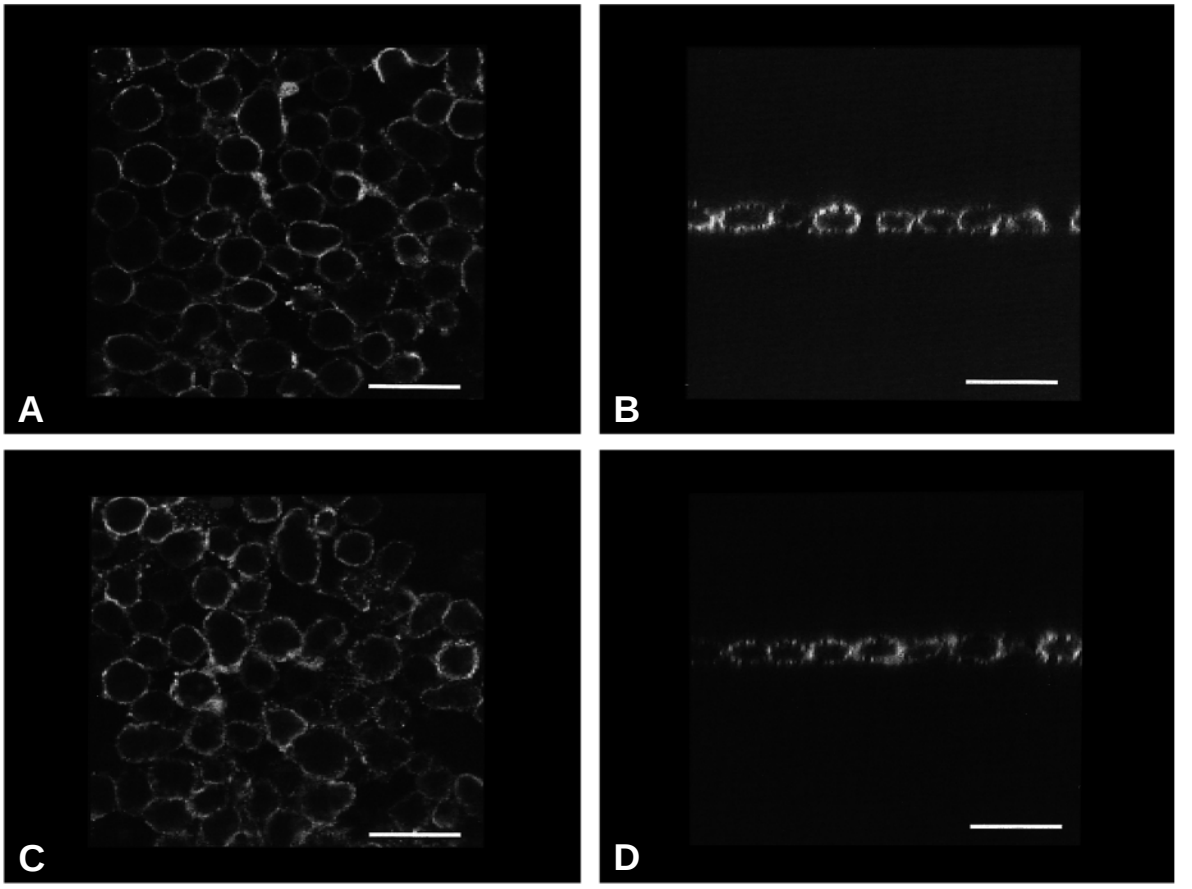

Fig. 3. Distribution of CD32 molecules on control and stimulated THP-1 cells. THP-1 cells were cultured on bare (A,B) or fibronectin-coated (C,D) glass without (A,B) or with (C,D) interferon-γ. They were then labeled to reveal CD32 epitopes and examined with a confocal microscope. Sections parallel (A-C) or perpendicular (B-D) to the substratum are shown. The distribution of CD32 molecules and cell shape were comparable in both samples. Bar, 20 μm.

immunofluorescence microscopy: as shown in Table 4, THP-1 cell stimulation with fibronectin and/or interferon-γ treatment resulted in a decrease of the expression of a sialyl-dependent CD43 epitope without significant change of a protein epitope.

Second, in order to test more stringently the hypothesis that CD43 alteration might be responsible for increased CD32 accessibility, THP-1 cells were exposed to fibronectin and interferon-γ for different periods of time before being compared to controls with respect to CD43 expression and dynamic uptake of anti-CD32-coated spheres. As shown in Fig. 5, decrease of sialyl-dependent CD43 epitope and increase of sphere capture efficiency occured concomitantly between 6 and 12 hours after stimulation.

Third, we looked for a correlation between CD43 expression and CD32 accessibility at the individual cell level. Thus, stimulated cells were made to bind anti-CD32-coated spheres under dynamic conditions and coverslips were gently removed from the flow chambers, then labeled with antibodies specific for CD43 (sialyl-dependent epitope) or CD18 (the integrin β2 chain used as a control).

Cells were then examined with quantitative fluorescence

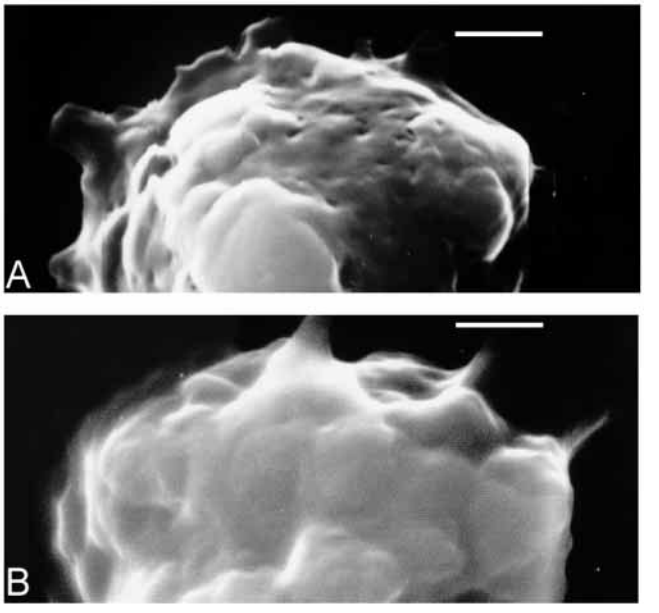

Fig. 4. Control and activated THP-1 cells display similar shape with limited roughness. THP-1 cells were cultured (A) on bare glass in standard medium (controls) or (B) on fibronectin-coated cells in culture medium supplemented with interferon-γ (stimulated cells). They were then fixed and studied with scanning electron microscopy. Representative images are shown. Bar, 1 μm.

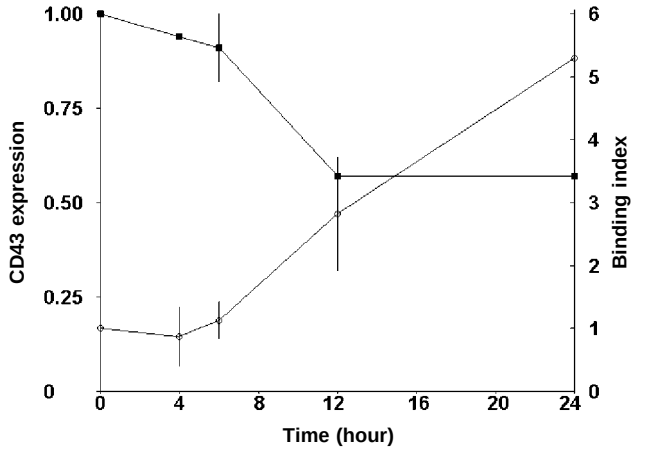

Fig. 5. Kinetics of adhesion increase and CD43 alteration in stimulated THP-1 cells. THP-1 cells were cultured (i) on bare glass in standard medium (controls) or (ii) on fibronectin-coated cells in culture medium supplemented with interferon-γ (stimulated cells). Cells were assayed for expression of a sialyl-dependent epitope of CD43 (right y axis, black squares) and dynamic uptake of anti-CD32-coated particles (left y axis, open squares). Three separate experiments were performed and the ratio between parameters measured on stimulated and control cells is shown as a function of the duration of stimulation A total number of 3,764 beads were monitored for adhesion measurements. Vertical bar length is twice the s.e.m calculated as described in Materials and Methods.

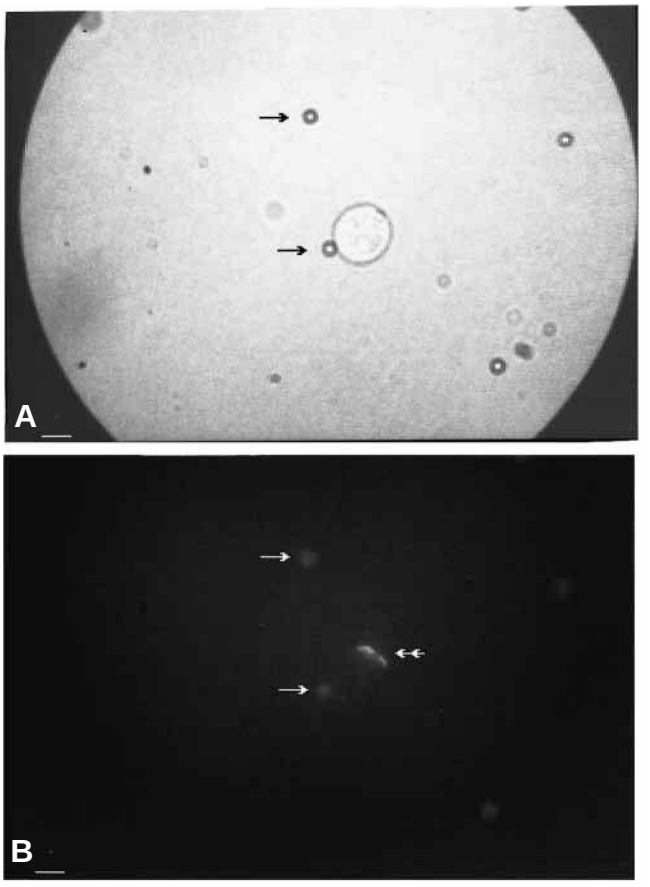

Fig. 6. THP-1 cell CD43 is depleted from the adhesion area after prolonged contact with test particles. Monocytic THP-1 cells were made to bind anti-CD32-coated spheres. Free and bound spheres are shown with arrows. After 45 minutes contact, cells were labeled with fluorescent anti-CD43 and examined with fluorescence microscopy. A typical image is shown with visible (A) and fluorescent (B) illumination. CD43 molecules (double arrow) are markedly redistributed at a distance from the contact area. Bar, 5 μm.

microscopy: Cells having bound at least one particle displayed 22% lower labeling than cells without any bound sphere, and this difference was higly significant ($P<0.01$) according to Student's *t*-test. On the contrary, the former cell population displayed only 7% lower labeling with anti-CD18, and this difference was not significant ($P>0.2$).

Particle binding results in delayed egress of CD43 from the contact area

A simple explanation for the finding that cell stimulation and CD43 alteration increased CD32 accessibility under dynamic, not under static conditions would be that cell-surface contact might expel bulky molecules from contact areas, thus resulting in time-dependent decrease of repulsion, which might make adhesion easier after prolonged contact. Indeed, it was recently reported that CD43 was depleted in regions of contact between THP-1 cells and immunoglobulin-coated erythrocytes (Soler et al., 1997) or T lymphocytes and antigen-presenting cells (Sperling et al., 1998). Thus, it was of interest to determine in the present study (i) whether contact between spheres and THP-1 cells could expel CD43 molecules from contact areas and (ii) whether such redistribution might be a limiting event in adhesion. Two series of experiments were performed to address this problem.

First, THP-1 cells were made to bind anti-CD32 coated cells for 45 minutes, then they were fixed and labeled for immunofluorescence study of the distribution of CD43. As exemplified in Fig. 6, adhesion triggered impressive depletion of CD43 in contact areas.

Second, the kinetics of CD43 redistribution was studied. THP-1 cells were labeled with fluorescein-derivatized anti-CD43, then deposited on the stage of a confocal microscope in a suspension of anti-CD32-coated spheres. Images were recorded at regular intervals. Cell areas were divided in six sectors whose relative fluorescence was determined in order to achieve a quantitative expression of fluorescence distribution. As exemplified in Fig. 7, fluorescence redistribution was indeed triggered by the uptake of beads, but this did not occur before about 10 minute contact, suggesting that no substantial reorganization could occur during a brief (less than 1 second) sphere-to-particle contact such as happened in the flow chamber during adhesion studies.

THP-1 cell stimulation involve selective removal of some particular carbohydrate species

It was interesting to know whether CD43 dyssialylation induced by cell stimulation was a limited and selective event, or most cell surface sugars were affected. Two series of experiments were performed to address this point.

First, electron microscopy was used to determine whether control and stimulated cells displayed apparent differences in the thickness of their pericellular matrices. Thus, cells were labeled with terbium (Fig. 8) and micrographs were studied

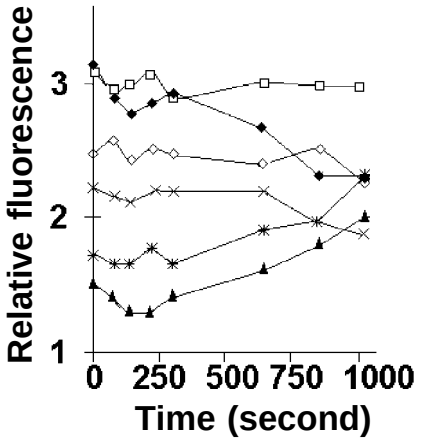

Fig. 7. Lack of CD43 redistribution during the first minutes following the uptake of anti-CD32-coated spheres by THP-1 cells. A suspension of anti-CD32-coated sphere was injected in a custom-made chamber whose floor was coated with adherent THP-1 cells. A representative field was chosen with a confocal microscope and an image was recorded every minute. Cells that bound a sphere during the experiment were selected and the heterogeneity of sector fluorescence was studied quantitatively with the sector procedure. Fluorescence distributions remained unaltered during several minutes. A representative example of a cell displaying reorganization of fluorescence is exemplified by plotting the time dependence of mean fluorescence of all sectors (note that the interaction area was located in sectors 4 and 5). Sectors 1, 2, 3, 4, 5 and 6 are represented by white losenges, white squares, black triangles, crosses, stars and black lozenges, respectively.

Table 5. lectin uptake by control and stimulated thp1 cells

	Fluorescence ratio stimulated/control	
Lectin	12 hours	24 hours
Peanut agglutinin	0.72±0.12	0.89±0.18
Concanavalin A	1.14±0.035	1.25±0.12
Lens culinaris hemagglutinin	1.19±0.14	0.97±0.06
Sambucus nigra agglutinin	1.07±0.16	1.03±0.11

THP-1 cells were maintained for 12 or 24 hours on glass surfaces in control medium (controls) or on fibronectin-coated glass in culture medium supplemented with interferon-γ. They were then labeled with fluorescent lectins and assayed for median fluorescence with a flow cytometer. The ratio between the fluorescences of stimulated and control cells was calculated. Mean values obtained in 3 separate sets of experiments are shown ± s.e.m.

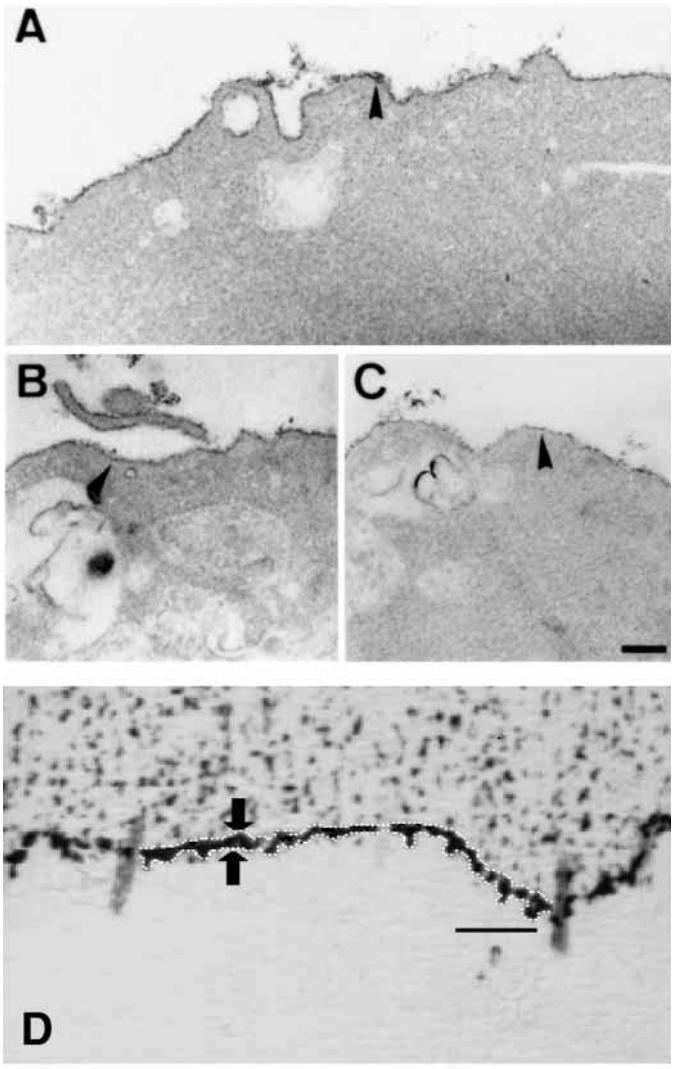

Fig. 8. Electron microscopical study of THP-1 cell glycocalyx. Monocytic THP-1 cells were stained with terbium chloride and examined with electron microscopy. The glycocalyx appeared as a dark lining (arrows). Control (A) and stimulated (B,C) cells are shown. Bar, 0.25 μm (for A,B,C). Micrographs were digitized with a hand scanner using maximum contrast setting, and the glycoxalyx boundaries were determined manually (as displayed with white dots, arrows). Contours were processed with a computer in order to determine the mean thickness of the dark region corresponding to the glycocalyx (D, bar, 0.1 μm).

quantitatively. The apparent glycocalyx thickness was indeed lower on stimulated cells (13.6±0.34 s.e.m.; n=58 segments) than controls (17.0±0.39 s.e.m.; n=63 segments). This 20% decrease was highly significant (P<0.001) according to Student's t-test.

Second, we asked whether all cell membrane oligosaccharides were affected in a similar way by the activation process. We tried to compare O-linked sugars (that are prominent on CD43) and N-linked carbohydrates. Also, it was of interest to determine whether sialic acid residues, that are often considered as anti-adhesive structures due to their negative charges, were strongly influenced by cell treatment. Thus, controls and stimulated cells were labeled with fluorescent lectins and assayed with flow cytometry. As shown in Table 5, after 12 hour stimulation, cells exhibited significantly (P<0.05) decreased labeling with peanut agglutinin (a ligand of terminal β galactose commonly used to label O-linked sugar chains; Galvan et al., 1998) and increased labeling with concanavalin A (a ligand of branched mannose residues composing N-linked sugar chains; Kobata, 1992). However, no significant variation of lens culinaris agglutinin was demonstrated. This lectin is known to bind a subclass of trimannosyl core groups found on N-linked oligosaccharides (Nemansky et al., 1998). Interestingly, *Sambucus nigra* agglutinin, a lectin specific for α2,6-linked sialyl groups that is a common structural motif on N-linked sugars (Razi and Varki, 1998) was bound to a similar exent by control and stimulated cells. Thus, glycocalyx reduction might essentially affect O-linked sugars or a subclass of these molecules.

Table 6. Effect of O-sialoglycoprotein endopeptidase on cell adhesive capacity and surface antigens

Experiment	Cell treatment	% Adhesion	Mean fluorescence after labeling with: Anti-CD43 (sialyl dependent)	Anti-CD32
I	-	21±3.5	57	6.1
	O-sialoglycoprotease	57±5.2 (P<0.0001)	28.3	4.8
II	-	26±3	66	5.0
	O-sialoglycoprotease	48±5 (P<0.0001)	29	3.6

In two series of experiments, control or O-sialoglycoprotease-treated THP-1 cells were assayed for (i) binding of anti-CD32-coated beads under flow, (ii) expression of CD43 sialyl-dependent epitope and (iii) CD32. Results of both experiments are shown. The number of beads used to determine each binding index ranged between 89 and 196. Standard errors and significance of enzyme treatment on adhesion was calculated as described in Materials and Methods.

Removal of O-linked oligosaccharides on THP-1 cells increases their dynamic binding capacity

These findings made it of interest to know whether a selective removal of O-linked sugars might result in adhesion increase. As shown in Table 6, cells treated with O-sialoglycoprotein endopeptidase displayed twofold increase of adhesion efficiency with concomitant diminution of the sialylated epitope of CD43.

DISCUSSION

The main purpose of this work was to demonstrate that living cells actually use glycocalyx modulation to regulate adhesiveness. Several lines of evidence support this conclusion:

First, it is important to rule out the possibility that the increased adhesion exhibited by stimulated THP-1 cells be due to an alteration of overall cell properties such as shape, spreading ability or membrane motility. Thus, extensive work suggested that cytoskeletal organization might influence adhesion efficiency (Lub et al., 1997; Stewart et al., 1998). Potential mechanisms might be regulation of cell membrane roughness (Willingham and Pastan, 1975), receptor distribution on the cell surface (vonAndrian et al., 1995) or of lateral mobility. Receptor mobility is indeed important to allow attachment strengthening by passive (diffusion driven) or active gathering into the adhesion area (Chan et al., 1991; André et al., 1990). These mechanisms are unlikely to affect our results since (i) control and activated THP-1 cells bound to the chamber floor were fairly smooth (Fig. 4) with comparable distribution of CD32 molecules (Fig. 3). (ii) the adhesion efficiency assayed with the flow chamber is unlikely to depend on active cell functions since a single molecular bond is thought to be able to make a particle stop (Pierres et al., 1998b), thus minimizing any requirement for receptor gathering or membrane smoothing. Indeed, as previously reported (Pierres et al., 1994) and checked with the present model (data not shown), binding probability is not affected by inhibitors of energy production. Also (Alon et al., 1997; Stockton et al., 1998), dynamic adhesion is probably too rapid to allow the involvement of signaling events: even with a low flow rate such as that used under our conditions, the relative velocity between the cells and the surfaces of interacting spheres was of order of 10 μm/second.

Thus, the duration of contact between a couple of adhesion molecules on interacting surfaces was of order of the ratio between molecular length and this velocity, i.e. about (10 nm)/(10 μm/second) = 0.001 second.

Second, the higher uptake of anti-CD32-coated spheres by stimulated THP-1 cells could not be ascribed to an increased epitope density, since control and stimulated cells bound similar amounts of anti-CD32 antibody (Table 2) and the same antibody was used to measure antigen density and mediate adhesion. This ruled out the possibility that cell stimulation might reveal some hidden epitope through a conformational change of CD32 (Tax and van de Winkel, 1990).

Third, we demonstrated a striking correlation between adhesion increase and modulation of the glycocalyx and particularly CD43: indeed, decrease of some carbohydrate epitopes of CD43 and adhesion increase occured simultaneously after the onset of stimulation, and this correlation was found at the individual cell level since an inverse relationship was found between adhesion and CD43 density. Thus, in combination with data shown in Table 6 and the previous finding that glycosidase treatment increased adhesion under flow (Sabri et al., 1995; Foa et al., 1996), the present results demonstrate that the increased adhesiveness of stimulated cells is due to increased receptor accessibility as a consequence of decreased cell coat thickness. An attractive hypothesis would be that the partial deglycosylation of CD43 might reduce molecular stiffness (Cyster et al., 1991; Jentoft, 1990) with concomitant decrease of protrusion from the bilayer level. Also, the decrease of surface charge that is likely to result from this deglycosylation might also decrease intermolecular repulsion within the glycocalyx, with concomitant thickness decrease. Note that the range of electrostatic repulsion between charged groups is of order of the Debye-Hückel reciprocal length, i.e. 0.8 nm in biological solutions, which is much lower than the length of adhesion molecules (Pierres et al., 2000). Thus, electrostatic repulsion is more likely to impair adhesion indirectly, through its potential effect on the swelling of the glycocalyx, than by directly inhibiting cell-cell approach.

Interestingly, a complete shedding of the cell coat is not required to increase adhesion efficiency. Indeed, 20% decrease of the apparent glycocalyx thickness, as estimated with electron microscopy, or 33% decrease of glycosylated CD43 epitopes was associated to fivefold increase of adhesion efficiency. Clearly, glycocalyx reduction might be a fairly convenient means for a cell to increase rapidly the activity of many tens of receptors borne by its membrane (Barclay, 1998), rather than simultaneously upregulating the activity of all these receptors. This mechanism might play a role in metastasis formation by tumor cells in view of the relationship between adhesive interactions and metastasis formation, and frequency of pericellular matrix alterations in transformed cells (Collard et al., 1986; Lloyd et al., 1996).

An obvious point of caution is that it is difficult to assess the validity of electron microscopical determination of glycocalyx thickness. Indeed, the possibility that specimen preparation might involve significant dimensional changes is well documented (King, 1991) and the glycocalyx might be particularly prone to such changes due to its fairly loose

structure. However, the validity of electron microscopical data is supported by the finding that interference reflection microscopy and electron microscopy yielded similar values for the distance between cells and adhesive substratum (Heath, 1992). Further, Foa et al. (1996) found that neuraminidase treatment decreased by 21% the width of the electron light gap separating adherent macrophages and red cells. The above data support the view that our electron microscopical study may yield at least a semi-quantitative estimate of glycocalyx thickness. Note that our reported value of a 13-17 nm range is comparable to the size of the CD32 molecule: the extracellular domain is made of 2 immunoglobulin domains, leading to an estimate of 8 nm for the total length (Springer, 1990b).

Another important conclusion from our experiments is that even slow motion can dramatically decrease the efficiency of cell adhesion receptors. Indeed, since about 1% of flowing anti-CD32-coated spheres were bound by THP-1 cells during their passage through the microscope field, while a sphere encountered about 10 cells, it may be estimated that only one thousandth of dynamic particle-to-cell encounters resulted in binding. This may be compared to about 50% efficiency in static conditions, where an average of one bead fell on each cell, since the bead/cell ratio was 1/1 and the major part of the glass surface was coated with cells. Thus, putatively important adhesive mechanisms may be uneffective in compartments such as airways, urinary tract, or lymphatic ways, and even the phagocytic uptake of bacteria subjected to brownian motion in resting medium may be much less efficient than in a pellet formed by centrifugation.

Several nonexclusive mechanisms might account for glycocalyx modulation. First, cell stimulation might alter carbohydrate metabolism (Montesano et al.,1984). Second, activation of cell surface proteases might result in cleavage of repulsive molecules with subsequent shedding (Rieu et al., 1992; Remold-O'Donnell and Parent, 1994, 1995). A third mechanism would be through the activation of a surface sialidase, as reported for activated B lymphocytes (Guthridge et al., 1994) as well as phagocytes (Lambré et al., 1990; Cross and Wright, 1991). This is in line with the present finding that CD43 was selectively dissialylated after THP-1 cell stimulation. Interestingly, this process might be fairly specific, since myeloid cell CD43 was reported to express α2,3-linked sialyl groups (Carlsson et al., 1986), while studies performed with lectins suggested that α2-6 sialyl groups were unaffected by THP-1 cell activation.

It is important to know whether CD43 is endowed with a particularly high anti-adhesive capacity. Indeed, following an estimate by Cyster et al. (1991), it is often considered that CD43 can cover nearly 20% of lymphoid cell surface (Ostberg et al., 1998). This figure was obtained by considering thymocytes as smooth spheres of 125 μm^3 volume (i.e. 3 μm radius and 113 μm^2 area), bearing 100,000 CD43 molecules viewed as elongated rods of 45 nm length and 5 nm diameter. If CD43 molecules are assumed parallel to the cell surface, the occupied area is indeed $100{,}000\times45\times5/10^6=22.5$ μm^2. However, if the anti-adhesive effect requires that CD43 be perpendicular to the cell surface (in order to extend 45 nm from the bilayer, as postulated by Cyster et al., 1991), the area covered by 57,000 molecules on a THP-1 cell would be only $\pi\times2.5^2\times57{,}000/10^6\approx1.1$ μm^2, i.e. 0.06% of the surface of a cell viewed as a sphere of 8.6 μm radius (not shown) with surface folds resulting in twofold higher area than a smooth sphere of comparable size. The concept that CD43 might be endowed with especially high repulsive potential is made attractive by the recent report that only CD43, not CD45, a molecule of comparable size, was depleted in areas of contact between T lymphocytes and antigen presenting cells (Sperling et al., 1998). Clearly, it would be interesting to compare the relative orientation of both molecular species with respect to the plasma membrane.

A final point is about the depletion of CD43 in cell-cell contact areas. Two consequences may be expected: first, this might allow progressive increase of cell-cell contact areas as observed during spreading or phagocytosis. second, molecular sorting in contact areas might be a prerequisite for the generation of signaling events (Shaw and Dustin, 1997)

This work was supported by a grant from the A.R.C. Electron microscopy was performed with the expert technical assistance of C. Allasia and M. Fraterno, Faculté de Médecine, Marseille. We thank Dr Remold O'Donnell for the kind gift of L10 antibody.

REFERENCES

Adams, D. O. and Hamilton, T. A. (1984). The cell biology of macrophage activtion. *Annu. Rev. Immunol.* **2**, 283-318.

Adams, D. O. and Hamilton, T. A. (1992). Molecular basis of macrophage activation: diversity and its origin. In *The Macrophage* (ed. C. E. Lewis and J. O'D. McGee), pp. 75-114, Oxford, IRL Press at Oxford University Press.

Alon, R., Chen, S., Puri, K. D., Finger, E. B. and Springer, T. A. (1997). The kinetics of L-selectin tethers and the mechanics of selectin-mediated rolling. *J. Cell Biol.* 13**8**, 1169-1180.

André, P., Benoliel, A. M., Capo, C., Foa, C., Buferne, M., Boyer, C., Schmitt-Verhulst, A. M. and Bongrand, P. (1990). Use of conjugates made between a cytolytic T cell clone and target cells to study the redistribution of membrane molecules in cell contact areas. *J. Cell Sci.* **97**, 335-347.

Ardman, B., Sikorski, M. A. and Staunton, D. E. (1992). CD43 interferes with T-lymphocyte adhesion. *Proc. Nat. Acad. Sci. USA* **89**, 5001-5005.

Auwerx, J. (1991). The human leukemia cell line, THP-1: a multifacetted model for the study of monocyte-macrophage differentiation. *Experientia* **47,** 22-31.

Barclay, A. N. (1998). Concluding remarks and the challenge from the immune system. *Faraday Discuss.* **111**, 345-350.

Bennett, H. S. (1963). Morphological aspects of extracellular polysaccharides. *J. Histochem. Cytochem.* **11**, 14-23.

Bevilacqua, M. P. and Nelson, R. M. (1993). Selectins. *J. Clin. Invest.* **91**, 379-387.

Brown, W. R., Barclay, A. N., Sunderland, C. A. and Williams, A. F. (1981). Identification of a glycophorin-like molecule at the cell surface of rat thymocytes. *Nature* **289**, 456-460.

Cai, T.Q. and Wright, S. D. (1995). Energetics of leucocyte integrin activation. *J. Biol. Chem.* **270**, 14356-14365.

Carlsson, S. R., Sasaki, H. and Fukuda, M. (1986). Structural variations of O-linked oligosaccharides present in leukosialin isolated from erythroid, myeloid and T-lymphoid cell lines. *J. Biol. Chem.* **261**, 12787-12795.

Chan, P. Y., Lawrence, M. B., Dustin, M. L., Ferguson, L. M., Golan, D. E. and Springer, T. A. (1991). Influence of receptor lateral mobility on adhesion strengthening between membranes containing LFA-3 and CD2. *J. Cell Biol.* **115**, 245-255.

Collard, J. G., Schijven, J. F., Bikker, A., La Rivière, G., Bolscher, J. G. M. and Roos, E. (1986). Cell surface sialic acid and the invasive and metastatic potential of T-cell hybridomas. *Cancer Res.* **46**, 3521-3527.

Cross, A. S. and Wright, D. G. (1991). Mobilization of sialidase from intracellular stores to the surface of human neutrophils and its role in stimulated adhesion responses of these cells. *J. Clin. Invest.* **88**, 2067-2076.

Cyster, J. G., Shotton, D. M. and Williams, A. F. (1991). the dimensions of the T lymphocyte glycoprotein leukosialin and identification of linear

protein epitopes that can be modified by glycosylation. *EMBO J.* **10**, 893-902.

Foa, C., soler, M., Fraterno, M., Passerel, M., Lavergne, J. L., Martin, J. M. and Bongrand, P. (1994). Electron microscopical analysis of cell-cell and cell-substrate interactions: use of image analysis, X-ray microanalysis and EFTEM. In *Studying Cell Adhesion* (ed. P. Bongrand, P. Claesson and A. Curtis), pp. 219-241, Heidelberg, Springer Verlag.

Foa, C., Soler, M., Benoliel, A. M. and Bongrand, P. (1996). Steric stabilization and cell adhesion. *J. Materials Sci. Materials in Medicine* **7**, 141-148.

Galvan, M., Murali-Krishna, K., Lau, L., Baum, L. and Ahmed, R. (1998). Alterations in cell surface carbohydrates on T cells from virally infected mice can distinguish effector/memory $CD8^+$ T cells from naive cells. *J. Immunol.* **161**, 641-648.

Guthridge, J. M., Kaplan, A. M. and Cohen, D. A. (1994). Regulation of B cell:T cell interactions: potential involvement of an endogeneous B cell sialidase. *Immunol. Invest.* **23**, 393-411.

Heath, J. P. (1992). Adhesions to substratum and locomotory behaviour of fibroblastic and epithelial cells in culture. In *Cell Behaviour* (ed. R. Bellairs, A. Curtis and G. Dunn), pp. 77-108. Cambridge University Press, Cambridge.

Jentoft, N. (1990). Why are proteins O-glycosylated ? *Trends Biochem. Sci.* **15**, 291-294.

King, M. V. (1991). Dimensional changes in cells and tissues during specimen preparation for the electron microscope. *Cell. Biophys.* **18**, 31-55.

Kobata, A. (1992). Structures and functions of the sugar chains of glycoproteins. *Eur. J. Biochem.* **209**, 483-501.

Lambré, C., R., Greffard, A., Gattegno, L., and Saffar L. (1990). Modifications of sialidase activity during the monocyte-macrophage differentiation in vitro. *Immunol. Lett.* **23**, 179-182.

Leblond, C. P. and Bennett, G. (1974). Elaboration and turnover of cell coat glycoproteins. In *The cell Surface in Development* (ed. A. A. Moscona), pp. 29-49. New York: J. Wiley and Sons.

Lee, G. M., Johnstone B., Jacobson, K.A. and Caterson, B. (1993). The dynamic structure of the pericellular matrix on living cells. *J. Cell Biol.* **123**, 1899-1907.

Lloyd, K. O., Burchell, J., Kudryashov, V., Yin, B. W. T. and Taylor-Papadimitriou, J. (1996). Comparison of O-linked carbohydrate chains in MUC-1 mucin from normal breast epithelial cell lines and breast carcinoma cell lines. *J. Biol. Chem.* **271**, 33325-33334.

Loftus, J. C. and Liddington, R. C. (1997). New insights into integrin-ligand interaction. *J. Clin. Invest.* **99**, 2302-2306.

Lub, M., van Kooyk Y., Vliet, S. J. and Figdor, C. G. (1997). Dual role fo the actin cytoskeleton in regulating cell adhesion mediated by the integrin lymphocyte function asociated molecule 1. *Mol. Biol. Cell* **8**, 341-351.

Lukacs, N. W., R. M. Strieter, V. Elner, H. L. Evanoff, M. D. Burdick and S. L. Kunkel. (1995). Production of chemokines, interleukin-8 and monocyte chemoattractant protein-1 during monocyte/endothelial cell interactions. *Blood* **86**, 2767-2773.

Manjunath, N., Correa, M., Ardman, M. and Ardman, B. (1995). Negative regulation of T-cell adhesion and activation by CD43. *Nature* **377**, 535-538.

Martinez-Palomo, A. (1970). The surface coats of animal cells. *Int. Rev. Cytol.* **29**, 29-75.

Michl, J. M., Pieczonka, M., Unkeless, J. C., Bell, G. I. and Silverstein, S. C. (1983). Fc receptor modulation in mononuclear phagocytes maintained on immobilized immune complexes occurs by diffusion of the receptor molecule. *J. Exp. Med.* **157**, 2121-2139.

Montesano, R., Mossaz, A., Ryser, J. E., Orci, L. and Vassalli, P. (1994). Leukocyte interleukins induced cultured endothelial cells to produce highly organized glycosaminoglycan rich pericellular matrix. *J. Cell Biol.* **99**, 1706-1715.

Nemansky M., Thotakura, N. R., Lyons, C. D., Ye S., Reinhold, B. B., Reinhold, V. N. and Blithe, D. L. (1998). Developmental changes in the glycosylation of glycoprotein hormone free alpha subunit during pregnancy. *J. Biol. Chem.* **273**, 12068-12078.

Ostberg, J. R., Barth, R. K. and Frelinger, J. G. (1998). The roman god Janus: a paradigm for the function of CD43. *Immunol. Today* **19**, 546-550.

Patel, K. D., Nollert, M. U. and McEver, R. P. (1995). P-selectin must extend a sufficient length from the plasma membrane to mediate rolling of neutrophils. *J. Cell Biol.* **131**, 1893-1902.

Pierres, A., Tissot, O., Malissen, B. and Bongrand, P. (1994) Dynamic adhesion of CD8-positive cells to antibody-coated surfaces: the initial step is independent of microfilaments and intracellular domains of cell binding molecules. *J. Cell Biol.* **125**, 945-953.

Pierres, A., Benoliel, A.M. and Bongrand, P. (1998a). Interactions between biological surfaces. *Curr. Opin. Colloid and Surface Sci*. **3**, 525-533.

Pierres, A., Benoliel, A. M. and Bongrand, P. (1998b). Studying Receptor-Mediated Cell Adhesion at the Single Molecule Level. *Cell Adhes. Commun.* **5**, 375-395.

Pierres, A., Benoliel, A. M. and Bongrand, P. (2000). Cell-cell interactions. In *Physical Chemistry of Biological Interfaces* (ed. A. Baszkin and W. Norde), pp. 459-522. Marcel Dekker, New York.

Rabinovitch, M., Manijas, R. E. and Nussenzweig, V. (1975). Phagocytosis paralysis induced by immune complexes. *J. Exp. Med.* **142**, 827-838.

Razi, N. and Varki, A. (1998). Masking and unmasking of the sialic acid-binding lectin activity of CD22 (Siglec-2) on B lymphocytes. *Proc. Nat. Acad. Sci. USA* **95**, 7469-7474.

Remold O'Donnell, E., Kennye, D. M., Parkman, R., Cairns, L., Savage, B. and Rosen, F. S. (1984). Characterisation of a human lymphocyte surface sialoglycoprotein that is defective in Wiskott-Aldrich syndrome. *J. Exp. Med.* **159**, 1705-1723.

Remold O'Donnell, E. and Rosen, F. S. (1990). Proteolytic fragmentation of sialophorin (CD43). Localization of the activation-inducing site and examination of the role fo sialic acid. *J. Immunol.* **145**, 3372-3378.

Remold O'Donnell, E. and Parent, D. (1994). Two proteolytic pathways for down-regulation of the barrier molecule CD43 of human neutrophils. *J. Immunol.* **152**, 3595-3605.

Remold O'Donnell, E. and Parent, D. (1995). Specific sensitifity of CD43 to neutrophil elastase. *Blood* **86**, 2395-2402.

Revel, J. P. and Karnovsky, M. J. (1967). Hexagonal array of subunits in intercellular junctions of the mouse heart and liver. *J. Cell Biol.* **33**, C12.

Rieu, P., Porteu, F., Bessou, G., Lesavre, P. and Halbwachs-Mecarelli, L. (1992). Human neutrophils release their major membrane sialoprotein, leukosialin (CD43) during cell activation. *Eur. J. Immmunol.* **22**, 3021-3026.

Rosengard, A. (1972). Probabilités et statistique en recherche scientifique. pp. 84-97. Paris, Dunod.

Rutishauser, U., Acheson, A., Hall, A. K., Mann, D. H. and Sunshine, J. (1988). The neural cell adhesion molecule (NCAM) as a regulator of cell-cell interactions. *Science* **240**, 53-57.

Sabri, S., Pierres, A., Benoliel A. M. and Bongrand, P. (1995). Influence of surface charges on cell adhesion: difference between static and dynamic conditions. *Biochem. Cell Biol.* **73**, 411-420.

Schwende, H., Fitzke, E., Ambs, P. and Dieter, P. (1996). Differences in the state of differentiation of THP-1 cells induced by phorbol ester and 1,25-dihydroxyvitamin D3. *J. Leukocyte Biol.* **59**, 555-561.

Shaw, A. S. and Dustin, M. L. (1997). Making the T cell receptor go the distance: a topological view of T cell activation. *Immunity* **6**, 361-369.

Silverman, L. B., Wong, R. L. K., Remold O'Donnell E., Vercelli, D., Sancho, J., Terhorst, C., Rosen F., Geha R. and Chatila, T. (1989). Mechanism of mononuclear cell activation by anti-CD43 (sialophorin) agonistic antibody. *J. Immunol.* **142**, 4194-4200.

Snedecor, G. W. and Cochran, W. G. (1980). Statistical Methods. pp. 124-128. Ames: The Iowa State University Press.

Soler, M., Merant, C., Servant, C., Fraterno, M., Allasia, C., Lissitzky, J. C., Bongrand, P. and Foa, C. (1997). Leukosialin (CD43) behavior during adhesion of human monocytic THP-1 cells to red blood cells. *J. Leuk. Biol.* **61**, 609-618.

Soler, M., Desplat-Jego, S., Vacher, B., Ponsonnet, L., Fraterno, M., Bongrand, P., Martin, J. M. and Foa, C. (1998). Adhesion-related glycocalyx study: quantitative approach with imaging-spectrum in the energy filtering transmission electron microscope (EFTEM). *FEBS Lett.* **429**, 89-94.

Sperling, A. I., Sedy, J. R., Manjunath, R., Kupfer, A., Ardman, B. and Burkhardt, J. K. (1998). Cutting edge: TCR signaling induces selective exclusion of CD43 from the T cell antigen-presenting cell contact site. *J. Immunol.* **161**, 6432-6462.

Springer, T. A. (1990a). The sensation and regulation of interactions with the extracellular environment: the cell biology of lymphocyte adhesion receptors. *Annu. Rev. Cell Biol.* **6**, 359-402.

Springer, T. A. (1990b). Adhesion receptors of the immune system. *Nature* **346**, 425-434.

Stockton, B. M., Cheng, G., Manjunath, N., Ardman, B. and vonAndrian, U. H. (1998). Negative regulation of T cell homing by CD43. *Immunity* **8**, 373-381.

Stewart, M. P., Mcdowall, A. and Hogg, N. (1998). LFA-1 mediated adhesion is regulated by cytoskeletal restraint and by a Ca^{2+} dependent protease, calpain. *J. Cell Biol.* **140**, 699-707.

Tax, W. J. and van de Winkel, G. J. (1990). Human Fc receptor II: a standby receptor activated by proteolysis ? *Immunol. Today* **11**, 308-310.

Tsuchiya, S., Kobayashi, Y., Goto, Y., Okumura, H., Nakae, S., Konno, T. and Tada, K. (1982). Induction of maturation in cultured human monocytic leukemia cells by a phorbol diester. *Cancer Res.* **42**, 1530-1536.

vonAndrian, U. H., Hasslen, S. R., Nelson, R. D., Erlandsen, S. L. and Butcher, E. C. (1995). A central role for microvillous receptor presentation in leukocyte adhesion under flow. *Cell* **82**, 989-999.

Wagner, R. C. and Chen, S. C. (1990). Ulstractructure distribution of terbium across capillary endothelium: detection by electron spectroscopic imaging and electron energy loss spectroscopy. *J. Histochem. Cytochem.* **38**, 275-282.

Willingham, M. C. and Pastan, I. (1975). Cyclic AMP modulates microvillus formation and agglutinability in transformed and normal mouse fibroblasts. *Proc. Nat. Acad. Sci. USA* **72**, 1263-1267.

Wright, S. D., Craigmyle, L. S. and Silverstein, S. C. (1983). Fibronectin and serum amyloid P component stimulate C3b- and C3bi-mediated phagocytosis in cultured human monocytes. *J. Exp. Med.* **158**, 1338-1343.

Yap, A. S., Brieher, W. M., Pruschy, M. and Gumbiner, B. M. (1997). Lateral clustering of the adhesive ectodomain: a fundamental determinant of cadherin function. *Curr. Biol.* **7**, 308-315.

Yauch, R. L., Felsenfeld, D. P., Kraeft, S. K., Chen L. B., Sheetz, M. P. and Hemler, M. E. (1997). Mutational evidence for control of cell adhesion through integrin diffusion/clustering independent of ligand binding. *J. Exp. Med.* **186**, 1347-1355.